VII International Conference on Computational Plasticity
COMPLAS 2003
E. Oñate and D.R.J. Owen (Eds)

3D FEM SIMULATION OF SHAPE ROLLING USING AN ALE METHOD

H. H. Wisselink*, J. Huétink†

*Netherlands Institute for Metals Research (NIMR)
P.O. Box 5008, 2600GA Delft, The Netherlands
e-mail: h.h.wisselink@ctw.utwente.nl, web page: www.nimr.nl

†University of Twente (UT)
Faculty of Engineering
P.O. Box 217, 7500AE Enschede, The Netherlands
e-mail: j.huetink@ctw.utwente.nl, web page: www.tm.ctw.utwente.nl/diekahome

Key words: ALE method, Shape rolling, 3D

Abstract. *The shape rolling of stator vanes has been modelled in 3D using the finite element method. Till now only the rolling of straight vanes, which have a constant cross section, is studied. Therefore this rolling process can be considered as a stationary process. Such processes can be described as a flow problem using the Arbitrary Lagrangian Eulerian (ALE) formulation. This makes it possible to follow free surfaces and to adapt the mesh in order to avoid large element distortions, to keep or create refinements were needed. The mesh topology however remains constant during a simulation. Topics of the ALE formulation such as mesh relocation, transfer of state variables etc. will be addressed in the paper.*

The tools are modelled as deformable bodies, as tool deformation is the most important reason for the deviation of the vane dimensions from the required dimensions. 3D FEM simulations have been carried out of the rolling of a test vane. Some characteristic results, such as material flow, tool deformations, stresses and strains, will be shown.

1 INTRODUCTION

A Dutch company manufactures stator vanes, a component of an aero engine. These stator vanes are produced with a cold shape rolling process out of a strip of sheet material as shown in Figure 1. This rolling process differs from the common shape-rolling process. In our case only one of the tools ("rolldie") rotates, the other tool ("dieplate") is flat and fixed. By applying horizontal and vertical forces the rolldie rolls over the dieplate deforming a strip of metal into a product.

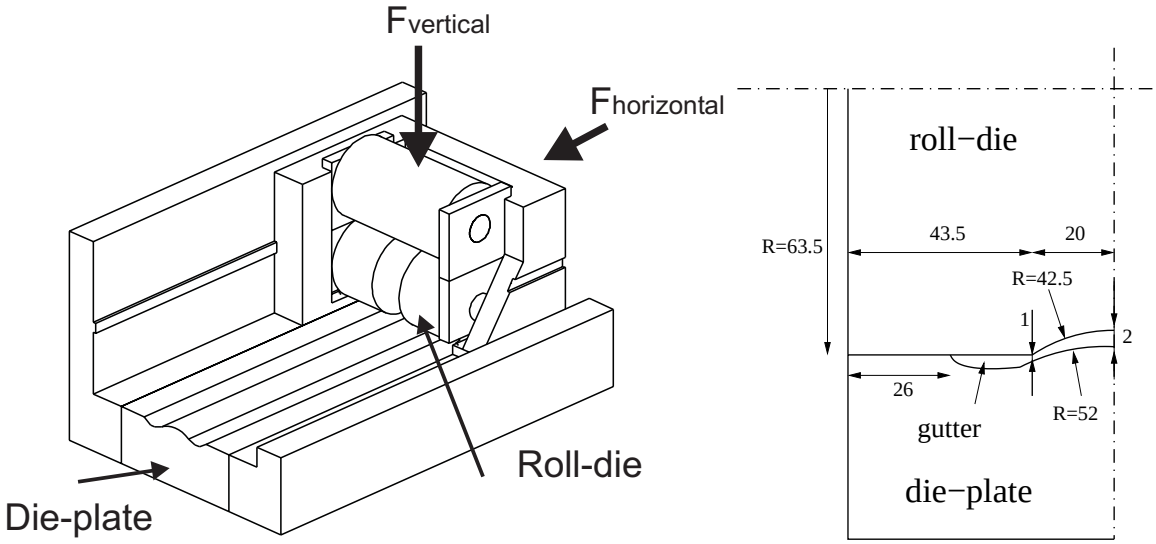

Figure 1: The investigated shape rolling process with tool dimensions [mm]

Neglecting the start and the end of a cycle, this process can be considered as a stationary process for vanes with a constant cross-section. Although the length of the vane to be rolled is limited to the perimeter of the rolldie, tests [1] demonstrated clearly a stationary region. When the material inside the dotted box is followed it becomes clear that the relative motions in the left and right part of Figure 2 are equal. The kinematics of the right part of Figure 2 will be used in our models.

Lateral spread of the strip is allowed by leaving some space at the edges. The rolling axis of the rolldie moves up and down during rolling (distance δ in Figure 3), depending on the process conditions as the applied loads, strip material, reduction and lubrication. The tools can even come into contact with each other at the edges for high loads, which is not unusual in practice. Also roll flattening will ocurr due to the applied loads. These tool deformations have to be taken into account in order to produce vanes within the required dimensional tolerances.

Sometimes expensive process redesign cycles are needed to meet the tight tolerances for the dimensions of the vanes. Therefore a finite element model is being developed to

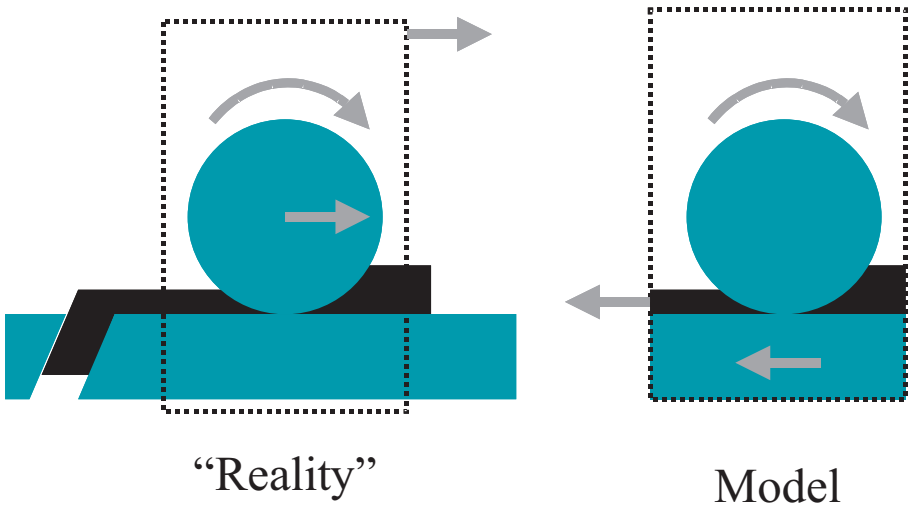

Figure 2: The relative motions during rolling.

get more insight in the mechanics of the process, which should support the design of new tools.

2 ALE method

The ALE method has proven to be an appropriate method for calculating the steady state of a stationary process, This has been shown for other processes as rolling (2D), extrusion and slitting [2, 3, 4, 5]. They used the finite element code DiekA, developed at the University of Twente, which contains an ALE formulation. The same approach will be applied to shape rolling in this paper.

The grid displacements are independent of the material displacements in the ALE formulation. Therefore it is possible to model the shape rolling process as a flow problem, while at the same time free surfaces can be followed and the element shape and size can be controlled. This gives the possibility to preserve a sufficient element quality and to add some adaptivity in case of large deformations. The element connectivity is not changed during the simulation. This limits the applicability of the ALE formulation to a domain, which does not change too much during the process. This requirement is fulfilled in case of stationary processes as the initial domain is chosen close enough to the expected steady state domain. During the simulation the material will flow through the domain. By following the free surfaces the domain (=mesh) will evolve from the initial state to the steady state. The relocation of the nodes, the definition of the grid displacement, is treated in Section 2.6. As the grid displacement is normally not equal to the material displacement a convection term has to accounted for. This topic is elaborated in Section 2.2

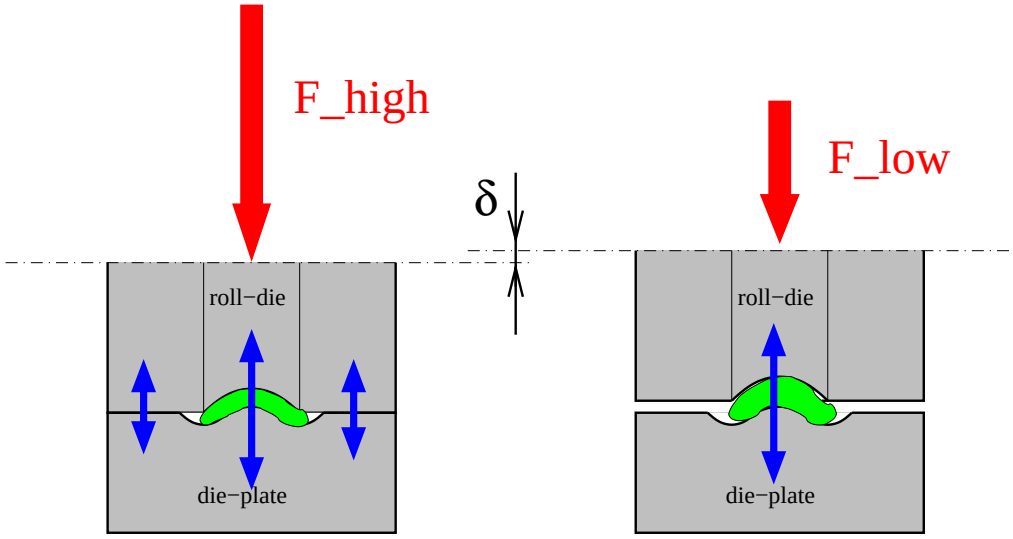

Figure 3: Mutual displacement of the tools

2.1 ALE formulations

Different approaches are possible to solve the ALE equations. Coupled [6, 7] or decoupled (= operator split) [8, 9, 10] ALE formulations are used normally. Here a semi-coupled ALE formulation is used [11, 5], which has similarities with both of the other approaches.

The semi-coupled ALE method can be seen as a coupled formulation in which the ALE predictor is replaced by a Updated Lagrangian (UL) predictor. With this UL predictor the material displacement increment is calculated as in a decoupled method. As the convective terms are neglected in the predictor a slower rate of convergence is expected compared to the coupled method.

The relocation of the nodes has to be performed in every iteration, which is less efficient than the decoupled method, where it is required once per step. But the flexibility is equal to the decoupled method. In the corrector part the convective increment is calculated using the values of the state variables at the beginning of the step, followed by the integration of the material increment.

Equilibrium is checked at the end of the time step and the iteration loop is repeated until the convergence criterion is fulfilled. This leads to a more robust algorithm, compared to the decoupled method, which is especially important in contact problems. Therefore the combination of robustness and flexibility is the main advantage of the chosen formulation.

2.2 Transfer of state variables

In case of an elasto-plastic material model the history dependent state variables (e.g. strain, stress or damage), which are known in the integration points, have to be calculated at the new position of the integration points. This convective increment has to be calculated at each step or iteration, depending on the ALE formulation used. It can be written as a convection or as an interpolation problem.

The convective increment is calculated with a weighed local and global smoothing scheme [11], although comparison of 2D convection schemes with the Molenkamp test [10, 12] showed that this scheme is not the most accurate one. The smoothing parameters, needed to keep the scheme stable, introduce some numerical diffusion. By taking sufficiently high values for the smoothing parameters in flow direction and low values perpendicular to the flow direction cross-wind diffusion can be reduced effectively. This will be illustrated in Section 3.

2.3 Contact

The contact between the tools and the material is an important factor in rolling processes. Therefore special contact elements are used to describe the contact between the strip and the tools [2]. These elements are based on a penalty formulation. Friction is modelled with a Coulomb law.

To calculate the tool deformation as well the tools as the strip are meshed. The nodes of the contact elements have to be connected to the nodes of the contacting bodies. In order to calculate a correct penetration distance, it is required that a pair of contact nodes is opposite to each other during the entire simulation. This gives an extra complication as the contacting surfaces should have an equal mesh. Therefore the meshing and relocation of the tools and the vane cannot be done independently. But using the ALE method it is possible for stationary processes, as was shown for a 2D rolling application [2]. It will be shown here that this is also possible for 3D applications.

2.4 Initial mesh

In the ALE method the initial and the final geometries are described with the same mesh topology. Therefore the choice of the initial mesh and the relocation of the mesh are closely related and already in the definition of the initial mesh must be anticipated for the expected final geometry.

It is chosen to create a mesh of hexahedrals with a constant topology in every cross-section perpendicular to the x-axis for the strip and the dieplate and a constant topology perpendicular to the z-axis for the rolldie. This results in regularly meshed free surfaces and "2D" meshes in every cross-section, which simplifies the mesh relocation.

We start by meshing the expected steady state geometry of the strip/vane. Having this mesh the tools can be meshed, such that the contact elements can be defined correctly. Due to symmetry only one half of the strip and tools has to be modelled. The initial

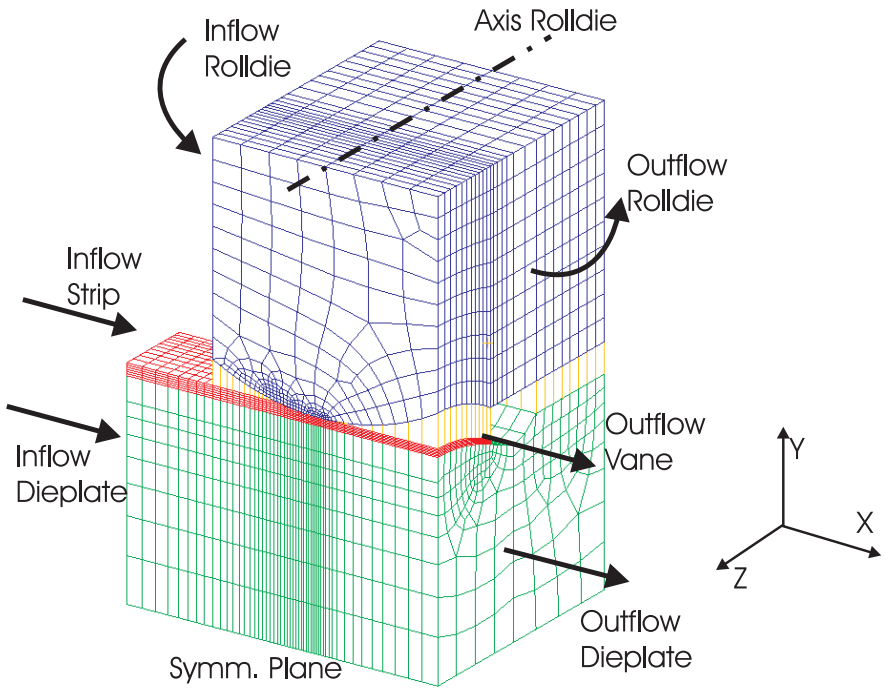

Figure 4: Initial mesh.

mesh is shown in Figure 4. Respectively 7748, 3640, 6006 and 1408 elements are used for the die-plate, strip, roll-die and contact.

2.5 Boundary and inflow conditions

A rotation is prescribed to the nodes on the horizontal plane through the axis of the roll-die. Because the vane is clamped to the dieplate, the same material displacement is prescribed to the outflow boundaries of the vane and the dieplate. The vertical rolling force is applied to the bottom face of the die-plate.

Inflow conditions are used at the inflow boundaries of the strip and dieplate. Here the stresses and strains are set to zero. No inflow conditions are used for the rolldie as proper conditions are hard to impose. This leads to an unstable solution at the inflow boundary of the rolldie: The stresses keep growing and a steady state will never be reached. However this is only a local effect which does not influence the results in the regions of interest.

2.6 Relocation of the nodes

The strategy and algorithms used for the relocation of the nodes in simulations of stationary shape rolling processes are given here. After the material displacement of the nodes has been calculated in the predictor the nodes are relocated such that the mesh displacement is zero in x-direction. At the same time the mesh follows the free surfaces in the y- and z- directions. The new positions of the nodes are determined in the following

order:

All surface nodes First all surface nodes are put back in the x-direction, keeping all nodes in "2D" cross-sections with a constant x-coordinate. The intermediate y- and z-coordinates are calculated with a convection scheme (Section 2.7).

Vane surface nodes Next the surface nodes of the vane are redistributed on the surface with the same convection scheme to keep or create refinements at the locations, where the largest deformations are found. The x-coordinate will not be changed here.

Tool surface nodes The surface nodes of the tools are repositioned such that they follow the movement of the surface nodes of the vane. Now the pairs of contact nodes connected to both surfaces will keep opposite to each other.

Internal nodes The new positions of the internal nodes can be calculated, when the new positions of all the surface nodes are known. They must follow the movements of the surface nodes in order to preserve a good element shape. This has been done with interpolation and smoothing techniques.

2.7 Accuracy of relocation

The determination of the new nodal positions of points on a grid line is an interpolation problem, which has the same characteristics as a convection problem. Therefore convection schemes will be used to calculate the new nodal positions using the positions of neighbouring surface nodes in flow direction.

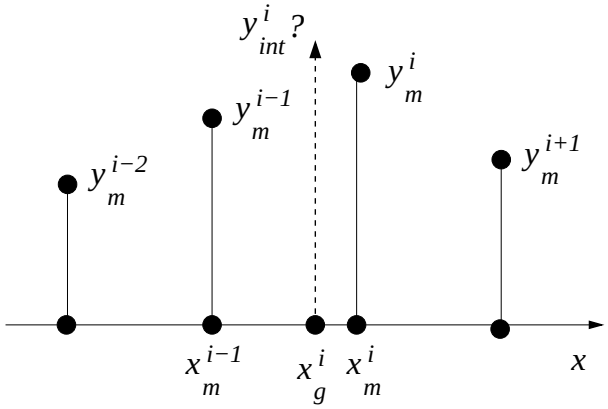

Figure 5: Convection of nodal coordinates in the x-direction.

First-order upwind schemes are known to be diffusive. A more accurate description of the boundary can be obtained with higher order interpolation or convection schemes.

Hence, a Lax-Wendroff scheme with van Leer limiters is used here, which shows no spurious oscillations.

$$\begin{aligned} y^i_{int} &= y^i_m - C\left(y^i_m - y^{i-1}_m\right) \\ &\quad -\frac{1}{2}C(1-C)\left[\psi(r_{i+1/2})(y^{i+1}_m - y^i_m) - \psi(r_{i-1/2})(y^i_m - y^{i-1}_m)\right] \end{aligned} \tag{1}$$

An intermediate y-coordinate y^i_{int} is calculated from y_m, the known y-coordinates after the predictor part. The same procedure is applied to calculate the intermediate z-coordinate. The van Leer limiter $\psi(r)$ stabilises the Lax-Wendroff scheme. In case of large gradients ($\psi(r) \to 0$) this scheme degenerates to the Upwind scheme. The influence of the limiter is small for small gradients, as the original Lax-Wendroff scheme is retained for $\psi(r) \to 1$.

$$r_{i+1/2} = \frac{y^i_m - y^{i-1}_m}{y^{i+1}_m - y^i_m}; \qquad r_{i-1/2} = \frac{y^{i-1}_m - y^{i-2}_m}{y^i_m - y^{i-1}_m}; \qquad \psi(r) = \frac{r + |r|}{1 + |r|} \tag{2}$$

The Courant number is determined directly from the material displacement in the x-direction. The new x-coordinate x^i_g is equal to the initial x-coordinate.

$$C = \frac{x^i_g - x^i_m}{x^i_m - x^{i-1}_m} \tag{3}$$

The application of this scheme in the x-direction is illustrated with a test contour. An initial sine shaped contour is shown in Figure 6. This contour is moving in the x-direction with a velocity of 0.1. The nodes on the contour are adapted using the described scheme. The results are shown after some steps. It can be concluded that the scheme is stable but also shows some diffusion.

The accuracy improves when the element size decreases. The Lax-Wendroff scheme has been derived for an equidistant grid. Therefore it is adapted a little to improve the accuracy at locations where mesh refinements have been used to reduce the amount of elements. However, the deterioration is small when neighbouring elements do not differ too much in size.

The final positions of the nodes are calculated from the intermediate values y^i_{int} and z^i_{int}. The convection scheme is used again for neighbouring surface nodes with equal x-coordinate. Now the Courant number is determined using a weight function [13], which makes it possible to control the element size. A simple weight function is used here which contains only the element length and a refinement factor. More sophisticated weight functions, containing the angles between elements and the values of the state variables, can be used but that makes it more difficult to control.

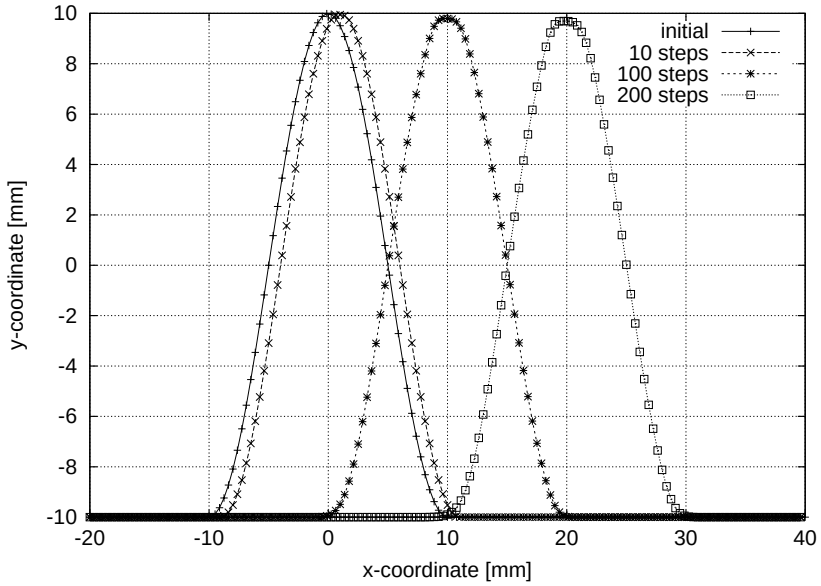

Figure 6: Contour of test problem.

2.8 Numerical issues

Up on increasing the number of elements and the number of time steps the calculation times get very large (days) for 3D shape rolling simulations. Therefore it becomes important to decrease the calculation times.

Furthermore the amount of available memory becomes insufficient for the use of direct solvers for large 3D simulations. Therefore iterative solvers have to be used. The used solvers, GMRES or BiCGSTAB with a SSOR preconditioner, provide acceptable answers using less time and memory.

The solutions for subsequent time steps in transient calculations that converge to a steady state are very similar. Therefore, the calculations can be speeded up if the predictor part of the first iteration is skipped. Instead, the converged solution of the last step is used as an initial guess of the material displacement increment.

This method proved to be unstable when the solution converged in one iteration per step. In that case only the corrector part is carried out, which is very fast, but the Newton-Raphson (NR) iterations will diverge in one of the subsequent steps. Therefore, at least two NR-iterations per step are required, which means that the solution will always be adapted. In that case the solution process is stabilised, except for abrupt changes in the material displacement increment, e.g. when points come into contact with the tools.

Line-searches are used in the second and next NR-iterations to improve the stability of the simulation.

3 RESULTS

In this section some results will be shown of the rolling of an aluminium strip of 40mm wide and 3mm thick with the tools of Figure 1. The material properties are given in Table 1. A standard elasto-plastic VonMises material model has been used for the strip and the tools. The steel tools remained elastic during the rolling of the relatively soft aluminium. The initial mesh is equal for all results shown (Figure 4). Only the vertical force and the friction coefficient are varied.

	AA 6061-O	tool steel
E-modulus [GPa]	70	217
ν	0.33	0.28
$\sigma_y(0)$ [MPa]	83	~ 2000
$\sigma_y(\varepsilon^p)$ [MPa]	$1 + 170(0.0261 + \varepsilon^p)^{0.2}$	—

Table 1: Material properties.

An example of the result of the mesh relocation procedure is shown in Figure 7. During the simulation the material flows through the mesh, but free boundaries are followed. This can clearly be seen at the development of the lateral spread. The element size is controlled such that the initial refinement in the regions with the highest deformations has been maintained. The mesh of the dieplate follows the nodal displacements of the mesh of the vane, keeping surface nodes opposite to each other.

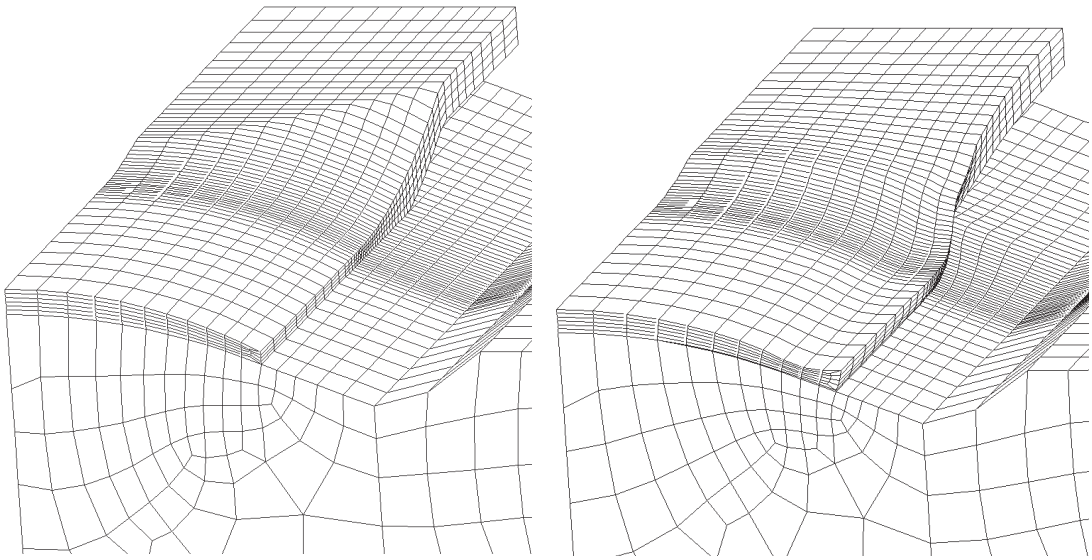

Figure 7: Initial (left) and steady state (right) mesh of the vane and the dieplate (F=600kN,μ=0.11)

As the nodal displacement is independent of the material displacement the meshes of Figure 7 give no information about the deformation of the material. Therefore the material flow is presented in Figure 8. Here the colors give material points which share the same origin for the vane and the dieplate.

(a) Particle tracing in z-direction.

(b) Particle tracing in x-direction.

Figure 8: Material flow for F=600kN (rolldie is not shown)

Figure 8(a) gives the lateral spread of the material. The material at the left (=symmetry plane) is compressed in z-direction. The material at the edge of the vane is elongated in z-direction. In Figure 8(b) the elongation of the strip and the relative motion between

strip and dieplate (the strip is pushed forward) can be seen. The material flow has been confirmed qualitatively by a series of rolling experiments with the same tools [1, 14].

From the figures with the material flow can be concluded that the deformation is homogeneous in large part of the domain. Only at the edges a non-homogeneous pattern can be found. Therefore problems with element distortion in Updated Lagrangian simulation might be expected there, especially upon element refinement. Main advantage of the ALE formulation compared with the Updated Lagrangian formulation is that the nodes have been relocated such that the mesh remains finest in the area with the largest elongation in z-direction. Also the elongation in rolling direction has no effect on the element size in that direction.

Figure 10 shows the influence of the vertical rolling force and the Coulomb friction coefficient on the reduction, spread and indirectly also the elongation of the vane. Cross-sections of the vane are given at x=0, which is straight below the axis of the rolldie. The thickness of the vane decreases and the spread increases with increasing rolling force and decreasing friction coefficient.

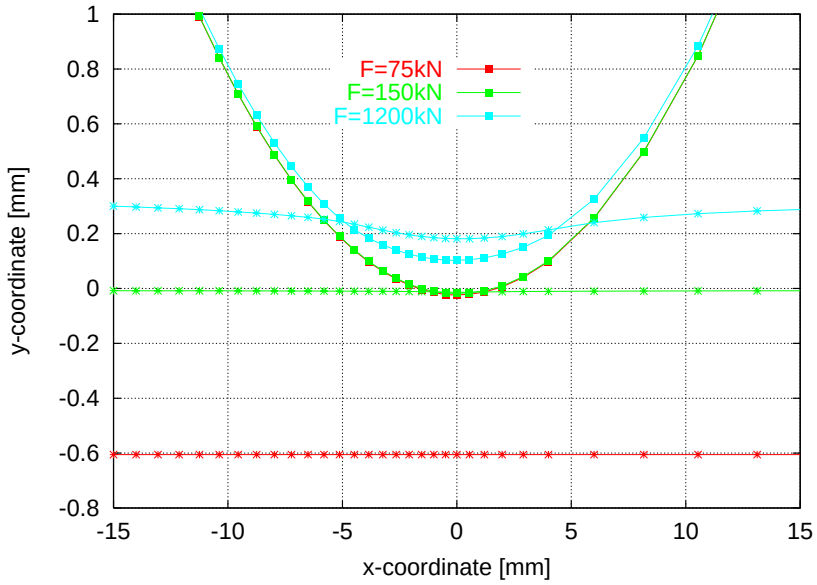

Figure 9: Influence of vertical rolling force on the tool deformation at z=0, ($\mu = 0.11$). $-*-=$ top surface dieplate and $-\blacksquare-=$ lower surface rolldie.

Except for the cases $F = 75kN, \mu = 0.11$ and $F = 150kN, \mu = 0.2$ the rolldie makes contact with the dieplate at the edges, as in Figure 3(left). The deformation of the tools is illustrated in Figure 9. This figure gives the outer contour of the tools at the edge, where the tools can make contact with each other. There is no contact for F=75kN, but for higher forces it can be seen that the tools deform and that the dieplate penetrates

into the rolldie. This is a result of the used penalty method to describe the contact (the contact elements in between the tools are not shown), which needs some penetration in order to give a reaction force. Some compromise has to be found between the allowed penetration and the calculation times, as higher values for the penalty deteriorate the convergence characteristics of the simulation. The accuracy of the simulations could be improved by better contact algorithms, e.g. augmented lagrangian methods.

The equivalent plastic strain is presented in Figure 11. This figure shows clearly that the cross-wind diffusion is very low. All contour lines remain straight after the material has passed the dieroll and no deformation is added anymore.

The yy-stress component in a vertical plane is given in Figure 12 for the vane and the tools. High compressive stresses are found in the vane and the tools.

4 CONCLUSIONS

The shape rolling of a stator vane has been simulated successfully in 3D. The ALE method is a suitable formulation for stationary processes as the element size can be kept small in the areas of interest. Furthermore it has been shown that the tool deformations can be included.

It has been indicated which parts of the simulations can be improved in order to get more accurate answers. Furthermore the calculation times for such 3D simulations should be decreased further for industrial use.

However the current model predicts all trends qualitatively correct and gives already much more insight in the investigated process.

REFERENCES

[1] A. Z. Abee. Rolling along the river. Technical report, University of Twente, 1999.

[2] J. Huétink, P. T. Vreede, and J. van der Lugt. The simulation of contact problems in forming processes using a mixed Eulerian-Lagrangian finite element method. In *Proc. NUMIFORM '89*, pages 549–554. A.A.Balkema, Rotterdam, 1989.

[3] H. G. Mooi. *Finite Element Simulations of Aluminium Extrusion.* PhD thesis, University of Twente, 1996.

[4] H. H. Wisselink. *Analysis of Guillotining and Slitting, Finite Element Simulations.* PhD thesis, University of Twente, 2000.

[5] H. H. Wisselink and J. Huétink. 3D FEM simulation of stationary metal forming processes with applications to slitting and rolling. Submitted for publication in Journal of Materials Processing Technology.

[6] W.K. Liu, H. Chang, J-S Chen, and T. Belytschko. Arbitrary Lagrangian-Eulerian Petrov-Galerkin finite elements for non-linear continua. *Comput. Methods Appl. Mech. Eng.*, 68:259–310, 1988.

[7] M.S. Gadala and J. Wang. Simulation of metal forming processes with the finite element method. *Int. J. Num. Meth. Eng.*, 44:1397–1428, 1999.

[8] D.J. Benson. An efficient, accurate, simple ALE method for nonlinear finite element programs. *Comput. Methods Appl. Mech. Eng.*, 72:305–350, 1989.

[9] F. P. T. Baaijens. An U-ALE formulation of 3-D unsteady viscoelastic flow. *Int. J. Num. Meth. Eng.*, 36:1115–1143, 1993.

[10] H. C. Stoker. *Developments of the Arbitrary Lagrangian-Eulerian Method in Non Linear Solid Mechanics, Applications to Forming Processes.* PhD thesis, University of Twente, 1999.

[11] J. Huétink. *On the simulation of thermomechanical forming processes.* PhD thesis, University of Twente, 1986.

[12] P. N. van der Helm, J. Huétink, and R. Akkerman. Comparison of artificial dissipation and limited flux schemes in Arbitrary Lagrangian Eulerian finite element formulations. *Int. J. Num. Meth. Eng.*, 41(6):1057–1076, 1998.

[13] J. P. Ponthot. The use of the Eulerian–Lagrangian FEM with adaptive mesh. applications to metal forming simulation. In *Computational Plasticity, Fundamentals and Applications: Proc.of the 3th Int. Conf.*, pages 2269–2280, 1992.

[14] H. H. Wisselink, J. Huétink, M.H.H. van Dijk, and A. J. van Leeuwen. 3D FEM simulations of a shape rolling process. In A.M. Habraken, editor, *Proc. 4th ESAFORM Conf.*, pages 843–846, 2001.

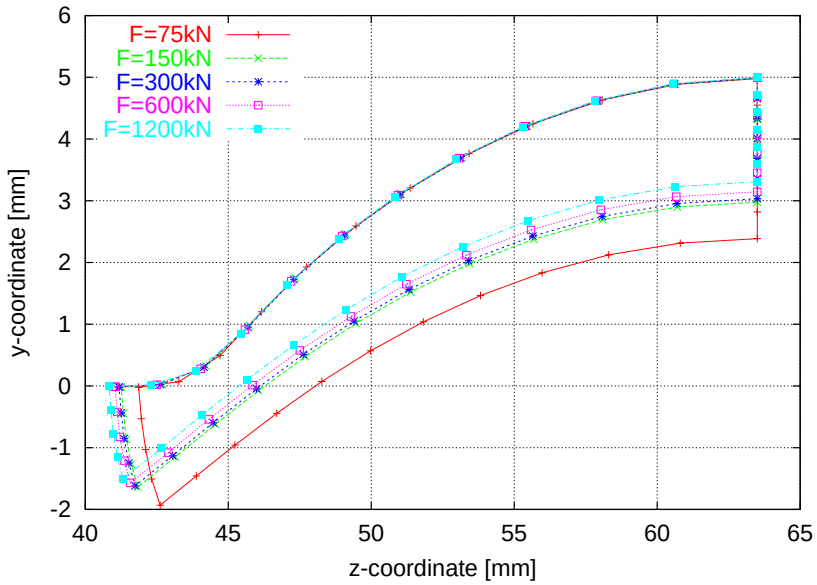

(a) Influence of vertical rolling force, $\mu = 0.11$.

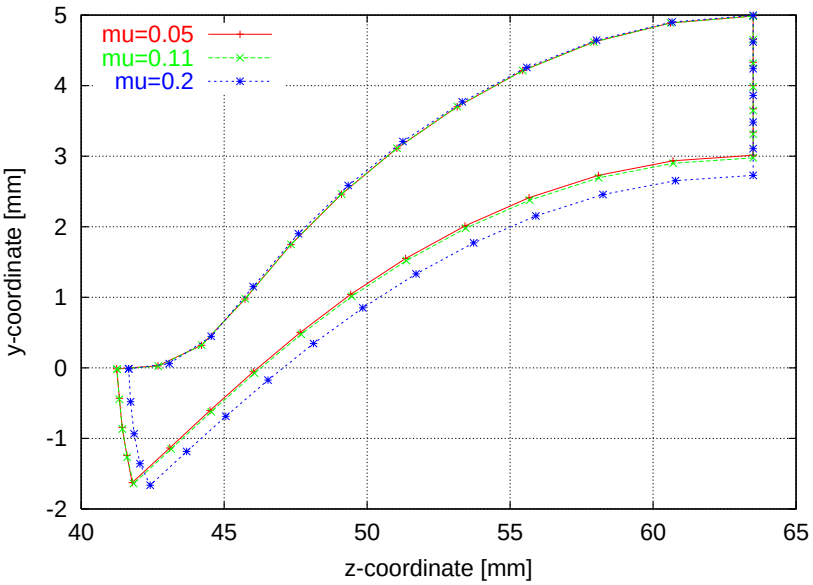

(b) Influence friction coefficient, F=150kN.

Figure 10: Vane dimensions at x=0.

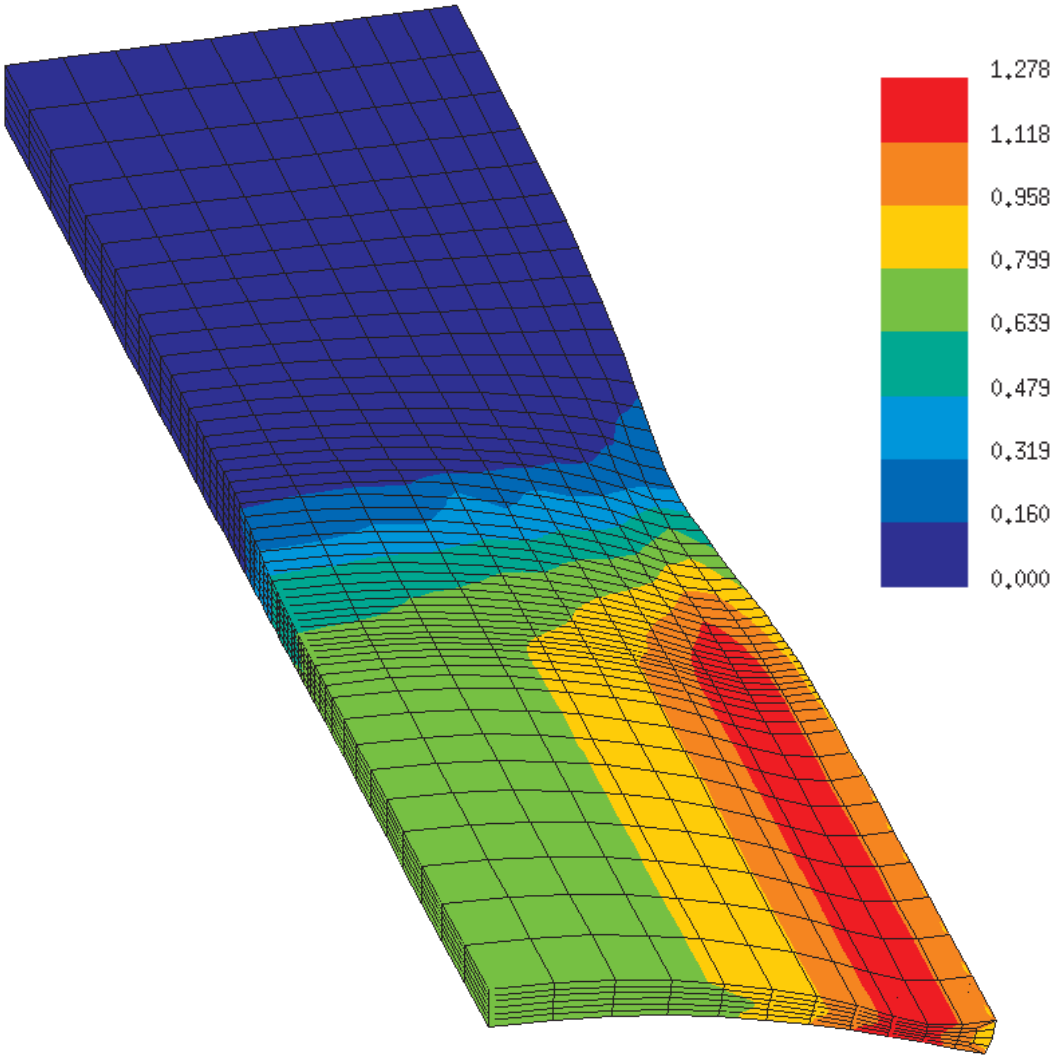

Figure 11: Equivalent plastic strain in the steady state for F=600kN (vane only).

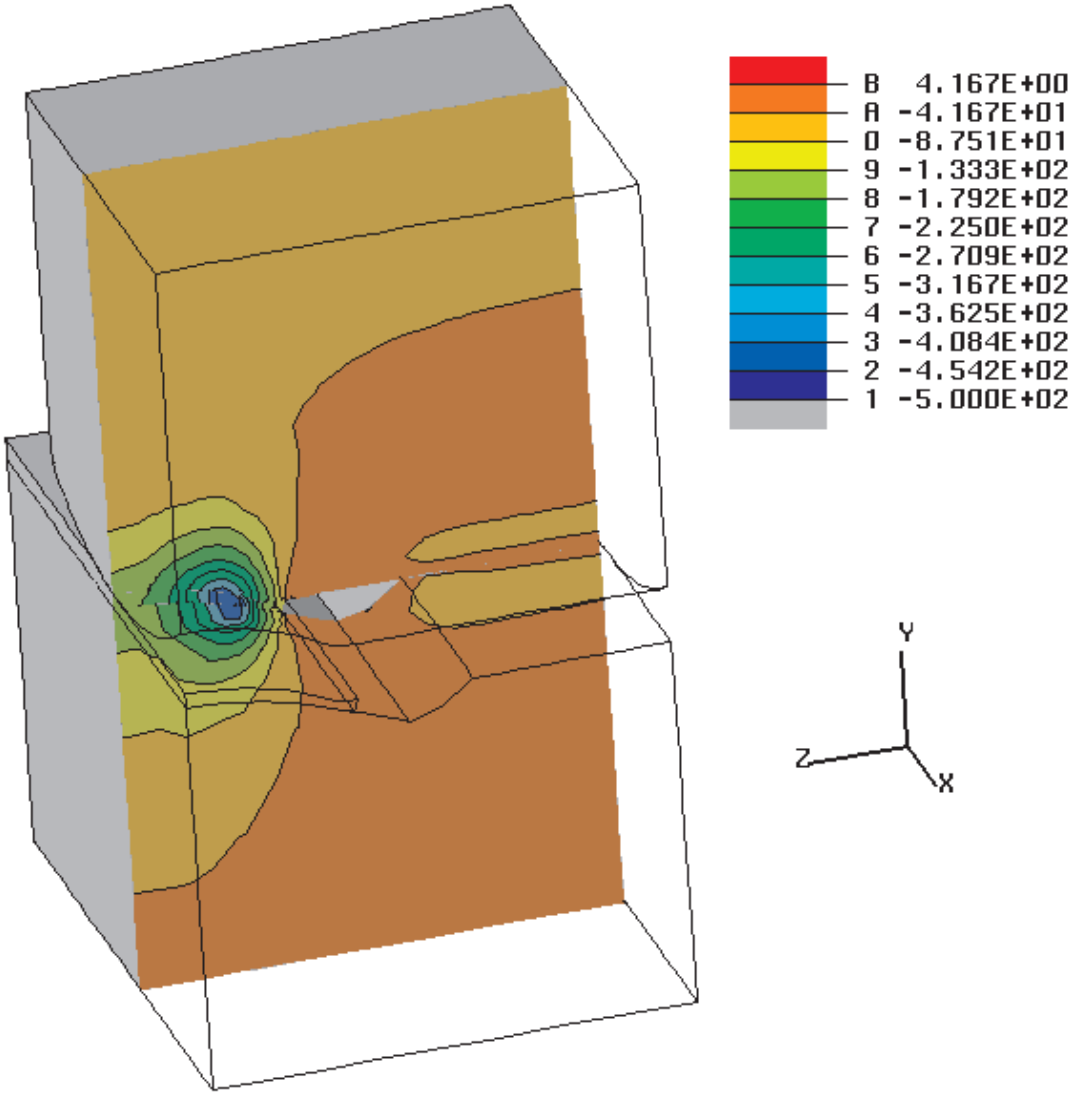

Figure 12: yy-stress [MPa] in the steady state for a cross-section at x=-2.0 (F=150kN).